Propagation and Amplification Dynamics of 1D Polariton Condensates

E. Wertz,[1] A. Amo,[1] D. D. Solnyshkov,[2] L. Ferrier,[1] T. C. H. Liew,[3] D. Sanvitto,[4,5] P. Senellart,[1] I. Sagnes,[1] A. Lemaître,[1] A. V. Kavokin,[6,7] G. Malpuech,[2] and J. Bloch[1,*]

[1]*CNRS-Laboratoire de Photonique et Nanostructures, Route de Nozay, 91460 Marcoussis, France*
[2]*Institut Pascal, PHOTON-N2, Clermont Université, University Blaise Pascal, CNRS, 24 avenue des Landais, 63177 Aubière Cedex, France*
[3]*Mediterranean Institute of Fundamental Physics, 31 via Appia Nuova, 00040 Rome, Italy*
[4]*NNL, Istituto Nanoscienze—CNR, Via Arnesano, 73100 Lecce, Italy*
[5]*Istituto Italiano di Tecnologia, Via Barsanti 73010 Lecce, Italy*
[6]*Physics and Astronomy School, University of Southampton, Highfield, Southampton SO171BJ, United Kingdom*
[7]*Laboratoire Charles Coulomb, CNRS-Universite de Montpellier II, Pl. Eugene de Bataillon, 34095 Montpellier Cedex, France*

(Received 5 July 2012; published 21 November 2012)

The dynamics of propagating polariton condensates in one-dimensional microcavities is investigated through time resolved experiments. We find a strong increase in the condensate intensity when it travels through the nonresonantly excited area. This amplification is shown to come from bosonic stimulated relaxation of reservoir excitons into the polariton condensate, allowing for the repopulation of the condensate through nonresonant pumping. Thus, we experimentally demonstrate a polariton amplifier with a large band width, opening the way towards the transport of polaritons with high densities over macroscopic distances.

DOI: 10.1103/PhysRevLett.109.216404 PACS numbers: 71.36.+c, 67.85.Hj, 78.55.Cr, 78.67.Pt

Optical amplifiers are devices with an active media capable of directly amplifying an optical signal traversing them. The medium is nonresonantly pumped, and amplification of a coherent propagating beam is obtained in a single passage by bosonic stimulated emission [1]. Such devices are important for the regeneration of fibered laser signals transmitted over long distances, or for high power lasers. Contrary to parametric amplifiers relying on four wave mixing, optical amplifiers based on nonresonant pumping have the great advantage of a large bandwidth and absence of phase matching restrictions.

Such a mechanism of optical amplification can in principle be used to regenerate a coherent population in other bosonic systems, for instance, to produce continuous matter-wave lasing in ultracold atomic Bose-Einstein condensates [2]. In an atom laser, a trapped Bose-Einstein condensate is coupled to an output mode, in which atoms flow away while keeping the coherence properties of the condensed state [3]. The duration of the atom laser is given by the size of the initial condensate and the outcoupling rate [4,5], and it could be extended by adding reservoir atoms feeding and amplifying the matter-wave condensate by bosonic stimulated relaxation. While some progress has been done in this direction [6], the continuous refilling of the ultracold atomic cloud remains experimentally challenging and, up to now, atomic lasers can only work in a pseudo-continuous mode with a finite duration.

Similar strategies can be considered for condensates of exciton-polaritons in semiconductor microcavities. Polaritons are mixed light-matter quasiparticles behaving as bosons in the low density limit [7]. Polariton condensates present a strong interest both for the study of the fundamental properties of quantum gases (superfluidity [8], quantised vortices [9] and dark [10] and bright [11] soliton formation have been reported), and for their potential functionalities as integrated optical elements. They present the flexibility of out of resonance optical excitation for their generation and, thanks to their interactions with uncondensed excitons, they can be easily accelerated, propagating over macroscopic distances [12,13]. Several works have proposed the use of such propagating polariton condensates to realize a polariton Berry phase interferometer [14] or various innovative spinoptronic devices [15–19] taking advantage of their nonlinear properties. However, the finite polariton lifetime (a few tens of picoseconds) results in the decay of the population along the propagation. This effect limits the region in which the polariton density is high enough for particle interactions to induce nonlinear phenomena. Thus, it is important to be able to amplify polariton condensates during their propagation.

In this Letter, we experimentally demonstrate polariton amplification by a reservoir of uncondensed excitons in a 1D microcavity. We monitor polariton propagation in a time resolved experiment. We show that the polariton condensate propagates with a group velocity that can be controlled varying the exciton-photon spectral detuning. Moreover, amplification is evidenced in the spatial region where excitons are nonresonantly injected: a strong increase of the emission is observed when polariton condensates traverse this region. This takes place due to bosonic stimulated relaxation of uncondensed polaritons, and it is well reproduced by solving a modified Gross-Pitaevskii equation

describing both the polariton condensate and the excitonic reservoir. Such polariton amplification opens the way to the implementation of cascadable polariton functionalities and optical transistor operation under nonresonant pumping.

The sample used in our experiments is described in detail in Ref. [12]. It consists in a high quality factor $\lambda/2$ planar cavity ($Q \sim 36\,000$) containing 12 GaAs quantum wells. Wire cavities with a width of 3.5 μm and a length of 200 μm were fabricated using electron beam lithography and reactive ion etching. The cavity wedge, present already in the planar structure, allows for the tuning of the bare exciton-photon energy difference $\delta = E_C - E_X$ of each wire. Within each wire, δ remains constant, as they are etched in the direction perpendicular to the wedge. Single microwires are excited nonresonantly (typically 100 meV above the lower polariton energy) with a Ti:sapphire laser delivering 2 ps pulses with a 82 MHz repetition rate. The laser is focused down to a 3 μm diameter spot with a microscope objective. The sample emission is collected through the same objective and imaged on the entrance slit of a streak camera coupled or not to a spectrometer in order to measure the time- and energy- or space-resolved polariton propagation. Momentum space is accessed by imaging the Fourier plane of the microscope objective taking advantage of the one-to-one relation between angle of emission and in-plane momentum of polaritons. All experiments are performed at 10 K.

Polariton condensation in such microwires has been reported under cw excitation [12] showing the formation of extended polariton condensates propagating out of the excitation region. Here, space- and time-resolved measurements allow direct monitoring of the propagation dynamics, as shown in Figs. 1(a)–1(d) for microwires with different exciton-cavity detunings under nonresonant pulsed pumping at $Y = 0$, in the middle of the wire. Below the condensation threshold [Fig. 1(a)] the emission dynamics is slow, reflecting the occupation of the excitonic reservoir [20], and very little propagation is observed: the emission remains localized in the area beneath the pulsed pump laser. The rise of the emission intensity apparent in the reported time window is given by the dynamics of exciton formation and relaxation into low momentum states [21,22]. Nonetheless, the total carrier population continuously decays in time.

At carrier densities above the condensation threshold (P_{th}), stimulated polariton relaxation gives rise to the formation of a condensate in the region of excitation at the bottom of the lower polariton branch with zero in-plane momentum ($k = 0$). At the high excitation densities reported in Figs. 1(b)–1(d) ($50P_{\mathrm{th}}$) the condensation takes place few picoseconds after the arrival of the excitation pulse ($t = 0$). The presence of an uncondensed excitonic reservoir in the excitation region induces a blueshift of the polariton energy (4 meV) caused by repulsive exciton-polariton interactions [12,23]. Since the excitonic reservoir remains localized in the region of excitation (because of the large exciton effective mass), no blueshift is generated outside this area. In this way, the reservoir induces an interaction energy that can be transformed into kinetic energy when the condensate exits the excitation region, resulting in the acceleration and propagation of the polariton condensate on both sides of this region, as observed in Figs. 1(b)–1(d). In the high excitation density case reported in Fig. 1, part of the condensate energy (~ 2.5 meV) is relaxed due to parametric polariton-polariton interactions, as reported in Ref. [24] (see also Ref. [25]). The rest of the interaction energy (~ 1.5 meV) is transformed into kinetic energy setting the condensate in movement.

Once the condensate exits the excitation spot, the propagation velocity remains constant and can be directly measured from the slope of the polariton trajectory in the real space-time resolved images [26]. The group velocity in the case of Fig. 1(b) is 1.8 μm ps^{-1}, and it is directly given by the kinetic energy. The group velocity is inversely proportional to the square root of the polariton mass, which is fixed by the curvature of the polariton dispersion [12]. Thus, by changing this curvature we can control the group velocity of the expelled polariton packets. This is shown in Figs. 1(b)–1(d) for three different detunings of $+3$, 0, and -10 meV, respectively. In all three cases we selected

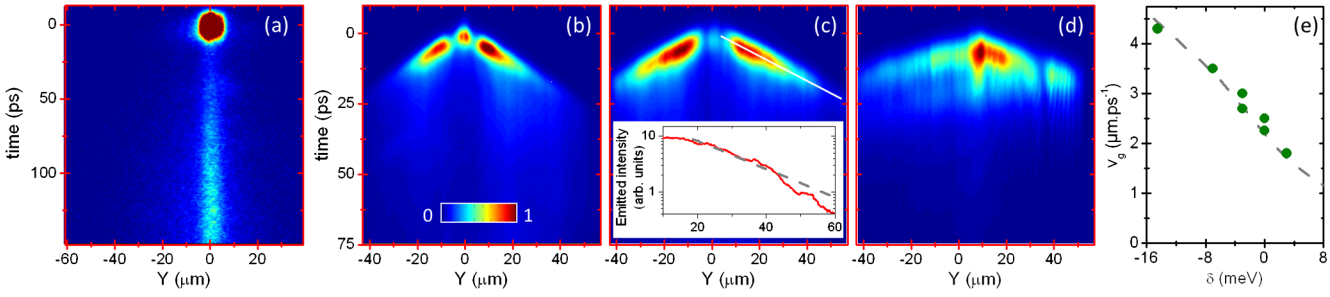

FIG. 1 (color online). Time resolved spatial distribution of the polariton emission below condensation threshold at $\delta = -3$ meV (a), and above condensation threshold at $\delta = +3$ meV (b), $\delta = 0$ meV (c), and $\delta = -10$ meV (d). In (b)–(d), the excitation density is chosen to produce ejected polariton condensates with a kinetic energy of 1.5 meV. The inset in (c) shows the decay of the polariton density along the white line (the dashed line is an exponential fit). (e) Measured polariton group velocity for different detunings (the dashed line is a guide to the eye).

excitation densities giving rise to the same kinetic energies for the ejected condensates (1.5 meV). When the detuning is decreased towards negative values, polaritons get lighter and the propagation speed increases, as summarized in Fig. 1(e).

The inset of Fig. 1(c) shows the characteristic decay of the density as the polariton wave packets propagate away from the excitation region (propagation length of ~ 17 μm). This decay is given by the photon lifetime in our etched microcavities, which is on the order of 15 ps, and evidences the need for an amplification or repumping of the condensate if propagation over longer distances is desired. We propose an amplification mechanism similar to that of optical amplifiers. It is based on the stimulated relaxation of the nonresonantly excited reservoir of excitons or polaritons to the bottom of the lower polariton branch, induced by the presence of a large polariton population in that state.

In order to experimentally prove polariton amplification, we place the excitation spot 35 μm away from one of the edges of the wire, as schematically represented in Fig. 2(a). Above threshold [$5P_{\mathrm{th}}$, Fig. 2(a)], the condensate is formed at $t_1 = 25$ ps after the arrival of the excitation pulse, and two condensates are ejected from the excitation region, one departing to the left [labeled (i)] and another one to the right [labeled (i′)]. When condensate i′ reaches the edge of the wire, it is reflected and propagates back. Remarkably, when it gets back to the pumped area (at $t_2 = 50$ ps) a strong increase of the emission signal is observed, accompanied by the propagation of two new condensate packets (ii and ii′), to the right and to the left of the region where the reservoir is located. The regeneration of the condensate takes place five times in our observation window.

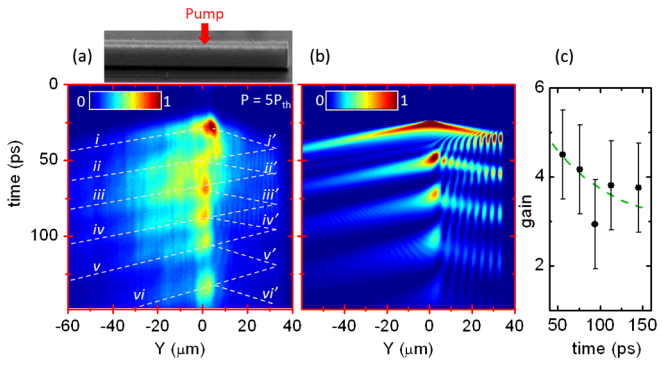

FIG. 2 (color online). (a) Time-resolved spatial distribution of the polariton emission at $5P_{\mathrm{th}}$ in a wire with $\delta = -3$ meV. The excitation spot is located 35 μm from the right edge of the wire. (b) Simulation considering polariton condensates propagating and interacting with the excitonic reservoir. (c) Measured amplification gain at each of the successive repopulations of the condensate; the green dotted line is an exponential fit with a decay of 300 ps. The modulation of the intensity observed both in (a) and (b) at $Y > 0$ arises from the interference between incoming and reflected condensates.

To evaluate the gain of the condensate amplification we first measure the intensity of the signal close to the edge of the wire ($Y = 32$ μm), and then we estimate from this value what the signal intensity would be without amplification at $Y = -15$ μm (considering only the polariton decay). Finally we take the ratio of this estimated intensity to the measured one at this very same position. The results are reported on Fig. 2(c), showing a gain of more than 4, and a time decay of the gain on the order of 300 ps (fitted dashed lines), compatible with that of the reservoir.

In order to understand in detail the amplification dynamics of the polariton signal, we study the reservoir induced blueshift and the emission energy of the subsequently expelled condensates. This is experimentally explored in Fig. 3(a), which shows the energy of the condensates traversing the region at $Y = -25$ μm on Fig. 2(a). At $t_1 = 25$ ps condensation takes place at $k = 0$ in the pumped region with an energy that is blueshifted by an amount $\Delta E_{\mathrm{i}} = 1.5$ meV with respect to the regions without reservoir [see Fig. 3(a)]. Note that in this case of moderate excitation density ($5P_{\mathrm{th}}$) polariton-parametric relaxation is negligible (contrary to the case of Fig. 1). ΔE_{i} corresponds to the condensate energy in the excitation region, given by the total reservoir population at t_1, and sets the kinetic energy of condensates i and i′ [12]. The reservoir induced interaction energy is thus fully converted into kinetic energy. At t_2, the reservoir population has partly decayed resulting in a decrease of the $k = 0$ energy in the region of excitation ($\Delta E_{\mathrm{ii}} = 1.3$ meV). The arrival in that region of the reflected condensate i′ induces a restimulation of the condensate from the reservoir, amplifying the

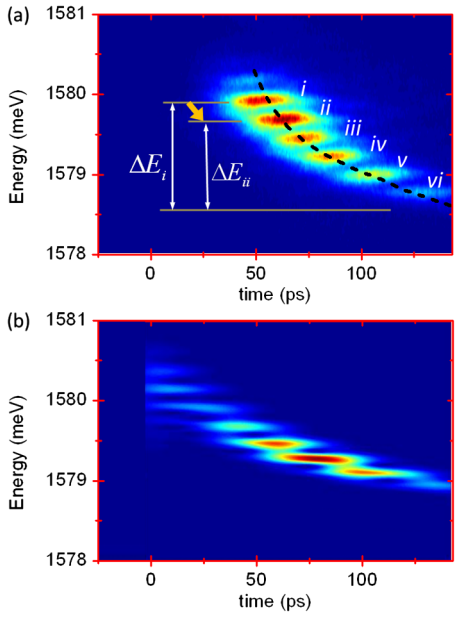

FIG. 3 (color online). Energy of the successive condensates as they pass through $Y = -25$ μm on Fig. 2(b): (a) measured experimentally and (b) simulated. The black dashed line is the measured energy at $k = 0$ under the excitation spot.

condensate density. This restimulation takes place simultaneously with the energy relaxation of condensate via polariton-reservoir pair scattering, down to the local potential energy set by the reservoir density at the time delay t_2 (orange arrow in Fig. 3).

The mechanism we have described presents strong similarities to that of an optical amplifier, in which bosonic stimulation takes place exactly to the same energy state as that of the incoming field, which acts a seed. In our case, stimulation takes place simultaneously with the inelastic relaxation of the incoming condensate. The cascade observed in Fig. 3 reflects the time evolution of the $k = 0$ energy in the excitation region [measured in dashed lines in Fig. 3(a)], sampled by the passage of the successive condensates. The relaxation of the condensate traversing the reservoir region is, thus, essential to account for this energy cascade. As ΔE sets the kinetic energy of the expelled condensates, the energy relaxation results in the slow down of the subsequent emitted condensates, as it can be observed from the increasing slope of the dashed lines in Fig. 2(a). We can model the coupled dynamics of the condensate and the reservoir, with the use of a modified Gross-Pitaevskii equation including terms for the restimulation and inelastic relaxation of the condensate [27,28] depending on the local reservoir density [25]. This model allows us to fully reproduce our results, as evidenced in Figs. 2(b) and 3(b), including the slow down of the successively amplified condensates.

The flexibility of the out-of resonant excitation provides supplementary control of the propagating condensates. If the initial injected density is high enough, polariton-polariton interactions close to the excitation area induce polariton scattering towards lower-energy states [24], as discussed for the case of Fig. 1. The situation with excitation close to the wire edge is shown in Fig. 4(a), where the condensate that is initially ejected towards the right has a smaller energy than the reservoir-induced barrier [29] and gets trapped between the excitation region and the edge of the wire [12,30], rebounding continuously between the two without appreciable energy loss [25]. The spatial oscillation of this polariton wave packet is well reproduced by our simulations when run with a high initial density [Fig. 4(b)].

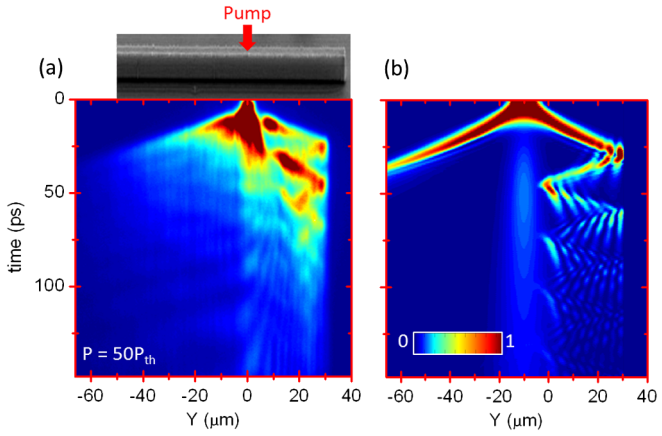

FIG. 4 (color online). Time resolved spatial distribution of the polariton emission at very high pump powers (50 times the condensation threshold) for a wire with $\delta = -3$ meV. The reservoir creates a potential barrier that cannot be crossed by the condensate: (a) measured experimentally and (b) simulated.

We have evidenced the amplification of polariton condensates under nonresonant excitation. The propagation with controlled velocity along with the repopulation process shown here, are two key ingredients to achieve transport of polariton condensates over macroscopic distances with a high density. Our scheme provides a large energy bandwidth for the re-populating beam, ranging from the gap energy of the employed quantum wells to the absorption energy of the materials constituting the Bragg mirrors of the cavity (from ~1.61 to 1.83 eV in our case). These are prerequisites for the implementation of a number of proposed functionalities based on the propagation of coherent polariton condensates [14–17,19,31]. In particular, our results open the way to their interconnection and cascadability, with the great advantage of being an out-of-resonance scheme not requiring the phase matching conditions of configurations based on parametric scattering [11,32,33].

This work was partly supported by the *RTRA Triangle de la Physique* "Boseflow1D", by the contract ANR-11-BS10-001 "Quandyde", by the FP7 *ITNs* "Clermont4" (235114) and "Spin-Optronics" (237252). T. L. was supported by the FP7 Marie Curie project EPOQUES (298811).

*jacqueline.bloch@lpn.cnrs.fr

[1] E. Desurvire, J. R. Simpson, and P. C. Becker, Opt. Lett. **12**, 888 (1987).
[2] M. Holland, K. Burnett, C. Gardiner, J. I. Cirac, and P. Zoller, Phys. Rev. A **54**, R1757 (1996).
[3] A. Öttl, S. Ritter, M. Köhl, and T. Esslinger, Phys. Rev. Lett. **95**, 090404 (2005).
[4] E. W. Hagley, L. Deng, M. Kozuma, J. Wen, K. Helmerson, S. L. Rolston, and W. D. Phillips, Science **283**, 1706 (1999).
[5] I. Bloch, T. W. Hänsch, and T. Esslinger, Phys. Rev. Lett. **82**, 3008 (1999).
[6] N. P. Robins, C. Figl, M. Jeppesen, G. R. Dennis, and J. D. Close, Nat. Phys. **4**, 731 (2008).
[7] J. Kasprzak, M. Richard, S. Kundermann, A. Baas, P. Jeambrun, J. M. J. Keeling, F. M. Marchetti, M. H. Szymanska, R. Andre, J. L. Staehli, V. Savona, P. B. Littlewood, B. Deveaud, and L. S. Dang, Nature (London) **443**, 409 (2006).
[8] A. Amo, J. Lefrère, S. Pigeon, C. Adrados, C. Ciuti, I. Carusotto, R. Houdré, E. Giacobino, and A. Bramati, Nat. Phys. **5**, 805 (2009).
[9] K. G. Lagoudakis, M. Wouters, M. Richard, A. Baas, I. Carusotto, R. Andre, L. S. Dang, and B. Deveaud-Pledran, Nat. Phys. **4**, 706 (2008).

[10] A. Amo, S. Pigeon, D. Sanvitto, V. G. Sala, R. Hivet, I. Carusotto, F. Pisanello, G. Lemenager, R. Houdre, E. Giacobino, C. Ciuti, and A. Bramati, Science **332**, 1167 (2011).
[11] M. Sich, D. N. Krizhanovskii, M. S. Skolnick, A. V. Gorbach, R. Hartley, D. V. Skryabin, E. A. Cerda-Mendez, K. Biermann, R. Hey, and P. V. Santos, Nature Photon. **6**, 50 (2012).
[12] E. Wertz, L. Ferrier, D. D. Solnyshkov, R. Johne, D. Sanvitto, A. Lemaitre, I. Sagnes, R. Grousson, A. V. Kavokin, P. Senellart, G. Malpuech, and J. Bloch, Nat. Phys. **6**, 860 (2010).
[13] G. Christmann, G. Tosi, N. G. Berloff, P. Tsotsis, P. S. Eldridge, Z. Hatzopoulos, P. G. Savvidis, and J. J. Baumberg, Phys. Rev. B **85**, 235303 (2012).
[14] I. A. Shelykh, G. Pavlovic, D. D. Solnyshkov, and G. Malpuech, Phys. Rev. Lett. **102**, 046407 (2009).
[15] T. C. H. Liew, A. V. Kavokin, and I. A. Shelykh, Phys. Rev. Lett. **101**, 016402 (2008).
[16] R. Johne, I. A. Shelykh, D. D. Solnyshkov, and G. Malpuech, Phys. Rev. B **81**, 125327 (2010).
[17] A. Amo, T. C. H. Liew, C. Adrados, R. Houdre, E. Giacobino, A. V. Kavokin, and A. Bramati, Nature Photon. **4**, 361 (2010).
[18] I. A. Shelykh, R. Johne, D. D. Solnyshkov, and G. Malpuech, Phys. Rev. B **82**, 153303 (2010).
[19] H. Flayac, D. D. Solnyshkov, and G. Malpuech, Phys. Rev. B **84**, 125314 (2011).
[20] J. Bloch and J. Y. Marzin, Phys. Rev. B **56**, 2103 (1997).
[21] T. C. Damen, J. Shah, D. Y. Oberli, D. S. Chemla, J. E. Cunningham, and J. M. Kuo, Phys. Rev. B **42**, 7434 (1990).
[22] J. Szczytko, L. Kappei, J. Berney, F. Morier-Genoud, M. T. Portella-Oberli, and B. Deveaud, Phys. Rev. Lett. **93**, 137401 (2004).
[23] L. Ferrier, E. Wertz, R. Johne, D. D. Solnyshkov, P. Senellart, I. Sagnes, A. Lemaitre, G. Malpuech, and J. Bloch, Phys. Rev. Lett. **106**, 126401 (2011).
[24] D. Tanese, D. D. Solnyshkov, A. Amo, L. Ferrier, E. Bernet-Rollande, E. Wertz, I. Sagnes, A. Lemaître, P. Senellart, G. Malpuech, and J. Bloch, Phys. Rev. Lett. **108**, 036405 (2012).
[25] See Supplemental Material at http://link.aps.org/supplemental/10.1103/PhysRevLett.109.216404 for a complete description of the model and additional results under high density excitation.
[26] T. Freixanet, B. Sermage, A. Tiberj, and R. Planel, Phys. Rev. B **61**, 7233 (2000).
[27] S. Choi, S. A. Morgan, and K. Burnett, Phys. Rev. A **57**, 4057 (1998).
[28] M. Wouters, T. C. H. Liew, and V. Savona, Phys. Rev. B **82**, 245315 (2010); M. Wouters, New J. Phys. **14**, 075020 (2012).
[29] T. Gao, P. S. Eldridge, T. C. H. Liew, S. I. Tsintzos, G. Stavrinidis, G. Deligeorgis, Z. Hatzopoulos, and P. G. Savvidis, Phys. Rev. B **85**, 235102 (2012).
[30] G. Tosi, G. Christmann, N. G. Berloff, P. Tsotsis, T. Gao, Z. Hatzopoulos, P. G. Savvidis, and J. J. Baumberg, Nat. Phys. **8**, 190 (2012).
[31] D. Ballarini, M. D. Giorgi, E. Cancellieri, R. Houdré, E. Giacobino, R. Cingolani, A. Bramati, G. Gigli, and D. Sanvitto, arXiv:1201.4071v1.
[32] A. Amo, D. Sanvitto, F. P. Laussy, D. Ballarini, E. del Valle, M. D. Martín, A. Lemaitre, J. Bloch, D. N. Krizhanovskii, M. S. Skolnick, C. Tejedor, and L. Viña, Nature (London) **457**, 291 (2009).
[33] C. Adrados, T. C. H. Liew, A. Amo, M. D. Martín, D. Sanvitto, C. Antón, E. Giacobino, A. Kavokin, A. Bramati, and L. Viña, Phys. Rev. Lett. **107**, 146402 (2011).